Where bio- meets geochemistry: Zooplankton gut passage mobilises lithogenic iron for ocean productivity

Katrin Schmidt[a,b,1], Christian Schlosser[c,d], Angus Atkinson[a,e], Sophie Fielding[a], Hugh J. Venables[a], Claire M. Waluda[a], Eric P. Achterberg[c,d]

[a]British Antarctic Survey, Madingley Road, High Cross, Cambridge CB3 0ET, UK

[b]Sir Alister Hardy Foundation for Ocean Science, The Laboratory, Citadel Hill, Plymouth PL1 2PB, UK

[c]Ocean and Earth Sciences, National Oceanography Centre Southampton, University of Southampton, Southampton SO14 3ZH, UK

[d]GEOMAR Helmholtz Centre for Ocean Research Kiel, Wischhofstr.1-3, 24148 Kiel, Germany

[e]Plymouth Marine Laboratory, Prospect Place, The Hoe, Plymouth PL1 3DH, UK

[1]corresponding author: E-mail: katsch@sahfos.ac.uk

Summary

Iron is an essential nutrient for phytoplankton, but low concentrations limit primary production and associated atmospheric carbon drawdown in large parts of the world's oceans [1,2]. Lithogenic particles deriving from aeolian dust deposition, glacial runoff or river discharge can form an important source, if the attached iron becomes dissolved and therefore bioavailable [3-5]. Acidic digestion by zooplankton is considered a potential mechanism for iron mobilisation [6], but evidence is lacking. Here we show that Antarctic krill sampled near glacial outlets at the island of South Georgia (Southern Ocean) ingest large amounts of lithogenic particles and contain three-fold higher iron concentrations in their muscle than specimens from off-shore, which confirms mineral dissolution in their guts. About 90% of the lithogenic- and biogenic iron ingested by krill is passed into their fecal pellets, which contain ~5-fold higher proportions of labile (reactive) iron than intact diatoms. The mobilised iron can be released in dissolved form via multiple pathways involving microbes, other zooplankton and krill predators. These pathways can deliver substantial amounts of bioavailable iron and therefore contribute to iron-fertilisation of coastal waters and the ocean beyond. In line with our findings, phytoplankton blooms downstream of South Georgia are more intensive and longer-lasting during years of high krill abundance on-shelf. Thus, zooplankton not only crop phytoplankton, but also boost new production via their nutrient supply. Understanding and quantifying iron mobilisation by zooplankton is essential to predict ocean productivity in a warming climate where lithogenic iron inputs from deserts, glaciers and rivers are increasing [7-10].

Results and Discussion

While most of the remote Southern Ocean is a high-nitrate low-chlorophyll (HNLC) area, primary productivity can be elevated for hundreds of kilometres downstream of islands, including South Georgia (Fig. 1A). This is considered a consequence of iron supply from the island shelves and its subsequent transport and recycling within the current flow [11-15]. Our *in situ* measurements of dissolved iron (DFe; < 0.2µm), total dissolvable iron (TDFe; unfiltered) and surface water salinity suggest that high iron concentrations over the northern shelf of South Georgia are also associated with a freshwater source: melting glaciers (Fig. S1). Glacial runoff has been found an important iron source in other polar regions [4,16,17], due to its high sediment load and the attached aggregations of iron oxyhydroxide nanoparticles [4,18]. However, most of the iron associated with glacial runoff is removed from surface waters during transition from low to high salinity [19], and the fate and chemical processing of iron during transport from glaciers to the adjacent ocean is not well understood [20].

Antarctic krill (*Euphausia superba*) is central to the South Georgia foodweb transferring primary production to higher trophic levels including fish, seals, penguins, albatrosses and whales [21]. Highest krill abundances on the eastern side of the island coincide with low chlorophyll *a* (chl *a*) concentrations and the dominance of fecal pellets in the suspended matter of surface waters, which indicates intensive grazing by krill (Fig. 1B-E). However, stomach content analysis reveals that krill do not only feed on phytoplankton but also ingest lithogenic particles and copepods when those are abundant (Fig. 1F). As a consequence, the amount of lithogenic particles in krill stomachs increased exponentially towards the main glacial outlets at Cumberland Bay, reaching >100 fold higher values than at a reference station ~170 km away (Fig. 2A). In concert with the increased ingestion of lithogenic particles, krill had up to three-fold higher iron concentrations in their muscle tissue and 1-2 orders of magnitude higher iron concentrations in their fecal pellets (Fig. 2B,C). Regardless of the sampling location, krill fecal pellets contained typically higher proportions of labile iron than the suspended material in surface waters [pellets: 2.4 ± 2.0%; suspended material dominated by diatoms: 0.5 ± 0.5% of total particulate iron, T-value = 4.85, *p*-value = 0.0001, DF = 31] (Fig.2D).

When feeding on lithogenic particles, both the enhanced iron concentrations in krill muscle tissue and the higher content of labile iron in krill fecal pellets compared to their food suggest that some of the lithogenic iron is mobilised and even dissolved during gut passage. Such a mechanism has been proposed previously [6] and shown for benthic- and intertidal species including annelids, bivalves and harpacticoid copepods [22-24], but until now evidence was missing for zooplankton. The mobilisation of lithogenic iron is likely due to the acidic digestion typical for crustaceans [25,26]. A gut pH of 5.4, as found in pelagic copepods [26], enhances the Fe(III) solubility ~100-fold compared to carbonate-buffered seawater [27]. Other factors associated with feeding such as mechanical- and enzymatic impact on particles, anoxia and the release of iron-binding ligands [22,26,28] may complement the effect of a lowered pH. However, the uptake of lithogenic particles during filter feeding is not restricted to Antarctic krill near glacial outlets, but is known from copepods, mysids, salps, other euphausiids and ciliates in river plumes, fjords, at the seabed or in the open ocean after dust deposition [29-35]. We therefore suggest that the mobilisation of lithogenic iron by zooplankton is a widespread phenomenon.

To quantify the role of iron mobilisation by krill in ocean fertilisation, individual iron release rates have to be measured and scaled up to the local abundance of krill. Only if the total iron release by krill covers a significant part of the phytoplankton iron demand, these processes can be considered important. Therefore, we conducted short-term shipboard incubations of krill as in a previous study [36], with the difference that not only TDFe release rates were measured [36] but also excretion rates of the bioavailable DFe. Stomach content analysis revealed that the DFe excretion rates increased with the initial amount of diatoms in krill stomachs [DFe = -25.07 + 3.59 (Diatoms), $R^2 = 0.624$, $p = 0.011$] (Fig. 2E), while the TDFe release rates were a function of both the amount of ingested diatoms and lithogenic particles [TDFe = -679 + 66.7 (diatoms) + 31.3 (lithogenic particles), $R^2 = 0.659$, $p = 0.025$, General Linear Model]. Moreover, there was a strong correlation between TDFe release rates and the dry mass of fecal pellets egested during 3 h-incubations, indicating that fecal pellets were the main source of the released TDFe (Fig. 2F). The total iron supply rates by krill in the upper mixed layer ranged from 0.1 to 31 pM DFe $d^{-1}$and 5 to 355 pM TDFe d^{-1}. These DFe excetion rates are at the

mid-range of values previously reported for micro- and mesozooplankton and covered up to 30% of the phytoplankton iron demand under bloom conditions (Table S1, S2). These are conservative estimates as on average two-thirds of the krill population resided below the mixed layer and additional DFe released by those krill may have entered surface waters through vertical transport [15].

Our study shows that on average >90% of iron ingested by krill is re-packaged into fecal pellets rather than excreted as DFe or incorporated into body tissue (Fig. 3). This is because iron concentrations were 3-4 orders of magnitude higher in krill fecal pellets than in muscle tissue and >90% of the iron released by krill during short-term incubations was in particulate rather than dissolved form. Therefore the cycling of iron ingested by krill is closely linked to the fate of their fecal pellets. We found on average 3.5 times (range: 0.1-17, median: 1.6 times) more fecal material at 150 m water depth than at 20 or 50 m, but in the upper depths pellets still accounted for high proportions of the suspended particulate matter (Fig. 1E). This suggests that even though many pellets sink to depth [37,38] and therefore export iron from surface waters, a substantial proportion remains in the upper mixed layer where intensive fragmentation and degradation occur [39,40] and iron is resupplied.

Regardless of the fate of these pellets, krill gut passage increases the proportion of labile iron and therefore the likelihood of subsequent iron dissolution due to either photochemical reactions, ligand activity, microbial recycling or zooplankton coprophagy [5,40-42]. Radiotracer experiments have shown that 6-96 pM DFe d^{-1} can be released from copepod fecal pellets, which is similar in extent to iron regeneration from phytoplankton either due to viral lysis or grazing [42]. Thus, in addition to immediate DFe excretion by krill, further DFe may derive from the degradation of fecal pellets and the digestion of krill tissue by predators [42,43]. In conclusion, krill uptake and mobilisation of lithogenic and biogenic iron provides the basis for several pathways of DFe supply. These pathways involve the activity of other organism - microbes, zooplankton, krill predators - as well as abiotic processes (Fig. 3), and in their sum they can deliver a substantial part of the phytoplankton iron demand.

In line with our findings, phytoplankton blooms downstream of South Georgia are more intensive and longer-lasting during years of high krill abundance on the shelf (Fig. 4A, Fig. S2). Correlations between median chl *a* concentration and annual krill abundance show negative slope values across the northern shelf, but positive values in the main bloom area further downstream (Fig. 4B). A negative relationship between krill density and phytoplankton abundance has previously been observed at the eastern side of South Georgia, and calculations confirmed that krill grazing rates exceeded the phytoplankton growth rates leading to 'top-down' control [45]. However, the here observed pattern of inverse correlations (negative on-shelf, positive downstream) suggests that high krill grazing pressure has a dual effect: in their main habitat it leads to substantial phytoplankton removal, but phytoplankton benefits from fertilisation after water masses have passed through this area. At our outermost sampling station, ~170 km downstream of the main glacial outlet, subsurface DFe and TDFe concentrations were still enhanced (0.9 nM DFe; 45 nM TDFe, Schlosser unpublished data) relative to HNLC waters (0.1 nM DFe; 3 nM TDFe) (9). Here, the Fe:C ratios of diatom-dominated suspended matter were 2 orders of magnitude higher (3600 ± 330 µmol Fe mol^{-1}) than values reported for diatoms under Fe replete conditions [46]. This indicates that high amounts of both DFe and TDFe can be transported away from South Georgia with the currents and aid subsequent phytoplankton development. Our study shows that iron mobilisation and recycling by krill, combined with the activity of other organisms, significantly enhances DFe supply and recycling in surface waters. Therefore we suggest a causal link between high krill feeding activities on the shelf and intensive, long-lasting phytoplankton blooms downstream.

There are undoubtedly other factors that contribute to the exceptional phytoplankton blooms downstream of South Georgia, e.g. shallow mixed layer depths, eddy activities, enhanced availability of macronutrients and luxury iron-uptake by abundant pennate diatoms [15, 47-49]. However, a state-of-the-art hydrodynamic-biogeochemical model without krill was unable to simulate the high chl *a* concentrations of the South Georgia bloom [50]. The discrepancy between observations and model output suggests that important mechanisms of bloom fertilisation were not addressed in the model. The mobilisation of lithogenic iron by zooplankton has rarely been considered [6], but our study

confirms the relevance of this mechanism, especially in regions with high zooplankton abundances such as South Georgia.

In conclusion, zooplankton grazers can play a unique role in the marine iron cycle. Firstly, they have efficient access to iron-rich material (e.g. lithogenic particles, large diatoms) and their acidic digestion does not only recycle iron but also lifts new iron from lithogenic sources into the foodweb. Secondly, zooplankton overlap spatially with phytoplankton and therefore the released iron can directly benefit primary production, while DFe from benthic sources [51,52] requires vertical transport into the euphotic zone. Third, zooplankton channel labile iron into fecal pellets which enhances the likelyhood of DFe release via microbial activity or coprophagy. Our study indicates that ocean fertilisation does not only depend on physical iron supply but also on the prevailing foodweb structure that facilitates iron mobilisation and recycling. We are only beginning to understand the complexity of these processes.

Experimental Procedures

This text summarises the methods used, with the *Supplemental Experimental Procedures* providing full details.

Sampling Our study took place during a research cruise at the northern shelf of South Georgia (Southern Ocean, 53-54°S; 35-39°W), from December 2010 to January 2011 onboard RRS *James Clark Ross.* The station activities included (1) an acoustic survey to estimate local krill densities over the diurnal cycle, (2) live krill sampling for stomach content analysis, fecal pellet production, iron measurements and incubation experiments, (3) collection of suspended particulate matter by Stand-Alone Pump Systems (SAPS) and CTD rosettes for taxonomic identification and iron measurements, (4) water sampling with towed fish and GO-FLO bottles for respective horizontal and vertical profiles of DFe and TDFe.

Krill incubations Under iron-clean conditions, freshly caught krill were rinsed and placed in 9L-polycarbonate carboys filled with 0.2 µm filtered seawater from surface-towed trace metal clean fish. At each station, 2-3 replicate carboys each containing 10-20 krill and 2 control carboys without krill were run at 2°C. The incubation water was sampled for DFe and TDFe initially, after 1h and 3h. At termination of the experiment, the remaining fecal pellets were collected for dry mass estimates.

Iron measurements In a trace metal clean laboratory container onboard ship, water samples for DFe (< 0.2 µm) and TDFe (unfiltered) were acidified with ultra pure HNO_3 to pH 1.66 for subsequent analysis by inductively coupled plasma-mass spectrometry (ICP-MS). The labile particulate iron fraction was remobilised with a 25% acetic acid solution at room temperature for 3h. The refractory particulate iron was digested in a mixture of concentrated HNO_3, HCl and HF acids at 140°C for 4 h. Both labile and refractory particulate iron were analysed by ICP-MS.

Author contributions

Conceptualization, K.S., A.A. and E.P.A.; Methodology, C.S., A.A., K.S. and S.F.; Investigation, C.S., A.A., K.S., S.F., H.J.V. and C.M.W.; Writing – Original Draft, K.S.; Writing – Review & Editing, K.S.,A.A., E.P.A. and C.S.; Funding Acquisition, A.A. , K.S. and E.P.A.

Acknowledgements

We thank the officers, crew and scientists onboard the RRS *James Clark Ross* for their professional support during JR247 and M. Patey for the SAPS deployment. E. Bazeley-White and H. Peat helped the acquisition of data from BAS- and NERC data bases, and M. Meredith supplied the drifter data. We are grateful to E. Young, M. Lohan, V. Kitidis and D. Bakker for discussing the results of our study. We acknowledge the MODIS mission scientists and associated NASA personnel for the production of data in the Giovanni online data system. This study was funded by the UK Natural Environment Research Council grant NE/F01547X/1.

205 **References**

206 **1.** Martin, J.H. (1990). Glacial-interglacial CO_2 change: the iron hypothesis. Paleoceanography *5*,
207 1-13.

208 **2.** Moore, C.M., Mills, M.M., Arrigo, K.R., Berman-Frank, I., Bopp, L., Boyd, P.W., Galbraith,
209 E.D., Geider, R.J., Guieu, C., Jaccard, S.L., et al. (2013). Processes and patterns of oceanic
210 nutrient limitation. Nature Geosci. *6*, 701-710.

211 **3.** Buck, K.N., Lohan, M.C., Berger, C.J.M., and Bruland, K.W. (2007). Dissolved iron
212 speciation in two distinct river plumes and an estuary: implications for riverine iron supply.
213 Limnol. Oceanogr. *52*, 843-855.

214 **4.** Raiswell, R., Tranter, M., Benning, L.G., Siegert, M., De'ath, R., Huybrechts, P., and Payne,
215 T. (2006). Contributions from glacially derived sediment to the global iron (oxyhydr)oxide
216 cycle: Implications for iron delivery to the oceans. Geochim. Cosmochim. Acta *70*, 2765-
217 2780.

218 **5.** Baker, A.R., and Croot, P.L. (2010). Atmospheric and marine controls on aerosol iron
219 solubility in seawater. Mar. Chem. *120*, 4-13.

220 **6.** Moore, R.M., Milley, J.E., and Chatt, A. (1984). The potential for biological mobilization of
221 trace elements from aeolian dust and its importance in the case of iron. Oceanologica Acta
222 *7(2),* 221-228.

223 **7.** Gordon, J.E., Haynes, V.M., and Hubbard, A. (2008). Recent glacier changes and climate
224 trends on South Georgia. Global. Planet Change *60*,72-84.

225 **8.** D'Odorica, P., Bhattachan, A., Davis, K.F., Ravi, S., and Runyan, C.W. (2013). Global
226 desertification: Drivers and feedbacks. Adv. in Water Resources *51*, 326-344.

227 **9.** Barker, A.J., Douglas, T.A., Jacobson, A.D., McClelland, J.W., Ilgen, A.G., Khosh, M.S.,
228 Lehn, G.O., and Trainor, T.P. (2014). Late season mobilisation of trace metals in two small
229 Alaskan arctic watersheds as a proxy for landscape scale permafrost active layer dynamics.
230 Chem. Geology *381*,180-193.

231 **10.** Gutt, J., Bertler, N., Bracegirdle, T.J.,Buschmann, A., Comiso, J., Hosie, G., Isla, E., Schloss,
232 I., Smith, G.R., Tournadre, J., and Xavier, J.C. (2014). The Southern Ocean ecosystem under
233 multiple climate change stresses – an integrated circumpolar assessment. Global Change
234 Biology. doi: 10.1111/gcb.12794
235 **11.** de Baar, H.J.W., de Jong, J.T.M., Bakker, D.C.E., Löscher, B.M., Veth, C., Bathmann, U., and
236 Smetacek, V. (1995). Importance of iron for plankton blooms and carbon dioxide drawdown in
237 the Southern Ocean. Nature *373*, 412-415.
238 **12.** Korb, R.E., Whitehouse, M.J., and Ward, P. (2004). SeaWiFS in the southern ocean: spatial
239 and temporal variability in phytoplankton biomass around South Georgia, Deep-Sea Res. II *51*,
240 99-116.
241 **13.** Blain, S., Quéguiner, B., Armand, L., Belviso, S., Bombled, B., Bopp, L., Bowie, A., Brunet,
242 C., Brussaard, C., Carlotti, F., et al. (2007). Effect of natural iron fertilisation on carbon
243 sequestration in the Southern Ocean. Nature *446*, 1070-1074.
244 **14.** Planquette, H., Statham, P.J., Fones, G.R., Charette, M.A., Moore, C.M., Slater, I., Nédélec,
245 F.H., Taylor, S.L., French, M., Baker, A.R., et al. (2007). Dissolved iron in the vicinity of the
246 Crozet Islands, Southern Ocean. Deep-Sea Res. II *54*, 1999-2019.
247 **15.** Nielsdóttir, M.C., Bibby, T.S., Moore, C.M., Hinz, D.J., Sanders, R., Whitehouse, M., Korb,
248 R., and Achterberg, E.P. (2012). Seasonal and spatial dynamics of iron availability in the
249 Scotia Sea. Mar. Chem. *130-131*, 62-72.
250 **16.** Gerringa, L.J.A., Alderkamp, A-C., Laan, P., Thuróczy, C-E., de Baar, H.J.W., Mills, M.M.,
251 van Dijken, G.L., van Haren, H., and Arrigo, K. R. (2012). Iron from melting glaciers fuels
252 the phytoplankton blooms in Amundsen Sea (Southern Ocean): Iron biogeochemistry. Deep-
253 Sea Res. II *71-76*, 16-31.
254 **17.** Hawkings, J.R., Wadham., J.L., Tranter, M., Raiswell, R., Benning, L.G., Statham, P.J.,
255 Tedstone, A., Nienow, P., Lee, K., and Telling J. (2014). Ice sheets as a significant source of
256 highly reactive nanoparticulate iron to the oceans. Nature Communications *5*, 3929, doi:
257 10.1038/ncomms4929.

18. Hopwood, M.J., Statham, P.J., Tranter, M., and Wadham, J.L. (2014). Glacial flour as a potential source of Fe(II) and Fe(III) to polar waters. Biogeochemistry doi:10.1007/s10533-013-9945-y.

19. Schroth, A.W., Crusius, J., Hoyer, I., and Campbell, R. (2014). Estuarine removal of glacial iron and implications for iron fluxes to the ocean. Geophys. Res. Lett. *41*, 3951-3958.

20. Zhang, R.F., John, S.G., Zhang, J., Ren, J.L., Wu, Y., Zhu, Z.Y., Liu, S.M., Zhu, X.C., Marsay, C.M., and Wenger, F. (2015). Transport and reaction of iron and iron stable isotopes in glacial meltwaters on Svalbard near Kongsfjorden: From rivers to estuary to ocean. Earth Planetary Sci. Lett. *424*,201-211.

21. Atkinson, A., Whitehouse, M.J., Priddle, J., Cripps, G.C., Ward, P., and Bandon, M.A. (2001). South Georgia, Antarctica: a productive, cold water, pelagic ecosystem. Mar. Ecol. Prog. Ser. *216*, 279-308.

22. Syvitski, J.P.M., and Lewis, A.G. (1980). Sediment ingestion by *Tigriopus californicus* and other zooplankton: mineral transformation and sedimentological considerations. J. Sedimentary Petrology *50*, 869-880.

23. Engelhardt, H.J., Brockamp, O. (1995). Biodegradation of clay-minerals – laboratory experiments and results from Wadden Sea tidal flat sediments. Sedimentology *42*, 947-955.

24. Needham, S.J., Worden, R.H., McIlroy, D. (2004). Animal-sediment interactions: the effect of ingestion and excretion by worms on mineralogy. Biogeosci. *1*, 113-121.

25. Dall, W., and Moriarty, D.J.W. (1983) Functional aspects of nutrition and digestion, p. 215-261. *In* L.H. Mantel [ed.], The biology of crustaceans, Vol. 5. Academic Press.

26. Tang, K.W., Glud, R.N., Glud, A., Rysgaard, S., and Nielsen, T.G. (2011). Copepod guts as biogeochemical hotspots in the sea: Evidence from microelectrode profiling of *Calanus* spp. Limnol. Oceanogr. *56*, 666-672.

27. Liu, X., and Millero, F.J. (2002). The solubility of iron in seawater. Mar. Chem. *77*, 43-54.

28. Sato, M., Takeda, S., and Furuya, K. (2007). Iron regeneration and organic iron(III)-binding ligand production during in situ zooplankton grazing experiment. Mar. Chem. 106, 471-488.

285 **29.** Tackx, M.L.M., Herman, P.J.M., Gasparini, S., Irigoien, X., Billiones, R., and Daro, M.H.
286 (2003). Selective feeding of *Eurytemora affinis* (Copepoda, Calanoida) in temperate estuaries:
287 model and field observations. Estuarine, Coastal and Shelf Sc. *56*,305-311.
288 **30.** Arendt, K.E., Dutz, J., Jónasdóttir, S.H., Jung-Madsen, S., Mortensen, J., Møller, E.F., and
289 Nielsen, T.G. (2011). Effects of suspended sediment on copepods feeding in a glacial
290 influenced sub-Arctic fjord. J. Plankton Res. *33*, 1526-1537.
291 **31.** Song, K.H., and Breslin, V.T. (1999). Accumulation and transport of sediment metals by
292 vertically migrating opossum shrimp, *Mysis relicta*. J. Great Lakes Res. *25*, 429-442.
293 **32.** Pakhomov, E.A., Fuentes, V., Schloss, I., Atencio, A., and Esnal, G.B. (2003). Beaching of the
294 tunicate *Salpa thompsoni* at high levels of suspended particulate matter in the Southern Ocean.
295 Polar Biol. *26*, 427-431.
296 **33.** Schmidt, K. (2010). Food and feeding in Northern krill (*Meganyctiphanes norvegica* SARS).
297 Adv. Mar. Biol. *57*, 127-171.
298 **34.** Schmidt, K., Atkinson, A., Steigenberger, S., Fielding, S., Lindsay, M.C.M., Pond, D.W.,
299 Tarling, G., Klevjer, T.A., Allen, C.S., Nicol, S., and Achterberg, E.P. (2011). Seabed foraging
300 by Antarctic krill: implications for stock assessment, bentho-pelagic coupling and the vertical
301 transfer of iron. Limnol. Oceanogr. *56*, 1411-1428.
302 **35.** Boenigk, J., and Novarino, G. (2004). Effect of suspended clay on the feeding and growth of
303 bacterivorous flagellates and ciliates. Aquat. Microb. Ecol. 34, 181-192.
304 **36.** Tovar-Sánchez, A., Duarte, C.M., Hernández-León, S., and Sañudo-Wilhelmy, S.A. (2007).
305 Krill as a central node for iron cycling in the Southern Ocean. Geophys. Res. Lett. *34*, L11601,
306 doi:10.1029/2006GL029096.
307 **37.** von Bodungen, B., Fischer, G., Nöthig, E-M., and Wefer, G. (1987). Sedimentation of krill
308 faeces during spring development of phytoplankton in Bransfield Strait, Antarctica. Mitt. Geol.
309 Paläontol. Inst. Uni. Leipzig *62*, 243-257.
310 **38.** Manno, C., Stowasser, G., Enderlein, P., Fielding, S., and Tarling, G.A. (2015). The
311 contribution of zooplankton faecal pellets to deep carbon transport in the Scotia Sea (Southern
312 Ocean). Biogeosci. *11*, 16105-16134.

39. González, H.E. (1992). The distribution and abundance of krill faecal material and oval pellets in the Scotia Sea and Weddell Seas (Antarctica) and their role in particle flux. Polar Biol. *12*, 81-91.

40. Belcher, A., Iversen, M., Manno, C., Henson, S.A., Tarling, G.A., and Sanders, R. (2016) The role of particle associated microbes in remineralization of fecal pellets in the upper mesopelagic of the Scotia Sea, Antarctica. Limnol. Oceanogr. *61*, doi:10.1002/lno.10269

41. Borer, P.M., Sulzberger, B., Reichard, P., and Kraemer, S.M. (2005). Effect of siderophores on the light-induced dissolution of colloidal iron(III) (hydr) oxides. Mar. Chem. *93*, 179-193.

42. Boyd, P.W., Strzepek, R., Chiswell, S., Chang, H., DeBruyn, J.M., Ellwood, M, Keennan, S., King, A.L., Maas, E.W., Nodder, S., et al. (2012). Microbial control of diatom bloom dynamics in the open ocean. Geophys. Res. Lett. *39*, L18601.

43. Nicol, S., Bowie, A., Jarman, S., Lannuzel, D., Meiners, K.M., and van der Merwe, P. (2010). Southern Ocean iron fertilization by baleen whales and Antarctic krill. Fish and Fisheries *11*, 203-209.

44. Meredith, M.P., Watkins, J.L., Murphy, E.J., Cunningham, N.J., Wood, A.G., Korb, R., Whitehouse, M.J., and Thorpe, S.E. (2003). An anticyclonic circulation above the Northwest Georgia Rise, Southern Ocean. Geophys. Res. Lett. *30(20)*, 2061. doi: 10.1029/2003GL018039.

45. Whitehouse, M.J., Atkinson, A., Ward, P., Korb, R.E., Rothery, P., and Fielding, S. (2009). Role of krill versus bottom-up factors in controlling phytoplankton biomass in the northern Antarctic waters of South Georgia. Mar. Ecol. Prog. Ser. *393*, 69-82.

46. Twining, B.S., Baines, S.B., Fisher, N.S., and Landry, M.R. (2004). Cellular iron contents of plankton during the Southern Ocean Iron Experiment (SOFeX). Deep Sea Res. I *51*, 1827-1850.

47. Whitehouse, M.J., Priddle, J., Brandon, M.A., and Swanson, C. (1999). A comparison of chlorophyll/ nutrient dynamics at two survey sites near South Georgia, and the potential role of planktonic nitrogen recycled by land-based predators. Limnol. Oceanogr. *44(6)*, 1498-1508.

48. Marchetti, A., Parker, S.M., Moccia, L.P., Lin, E.O., Arrieta, A.L., Ribalet, F., Murphy, M.E.P., Maldonado, M.T., and Armbrust, E.V. (2008). Ferritin is used for iron storage in bloom-forming marine pinnate diatoms. Nature *457*, 467-470.

49. Venables, H., and Moore, C.M. (2010). Phytoplankton and light limitation in the Southern Ocean: Learning from high-nutrient, high chlorophyll areas. J. Geophys. Res. *115*, C02015, doi:10.1029/2009jc005361.

50. Borrione, I., Aumont, O., Nielsdóttir, M.C., and Schlitzer, R. (2014). Sedimentary and atmospheric sources of iron around South Georgia, Southern Ocean: a modelling perspective. Biogeosci. *11*,1981-2001.

51. Elrod, VA, Berelson, WM, Coale, KH, and Johnson, K.S. (2004). The flux of iron from continental shelf sediments: a missing source for global budgets. Geophys. Res. Lett. *31*, L12307.

52. Wehrmann, L.M., Formolo, M.J., Owens, J.D., Raiswell, R., Ferdelman, T.G., Riedinger, N., and Lyons, T.W. (2014). Iron and manganese speciation and cycling in glacially influenced high-latitude fjord sediments (West Spitsbergen, Svalbard): Evidence for a benthic recycling-transport mechanism. Geochimica et Cosmochimica Acta 141, 628-655.

Figure legends

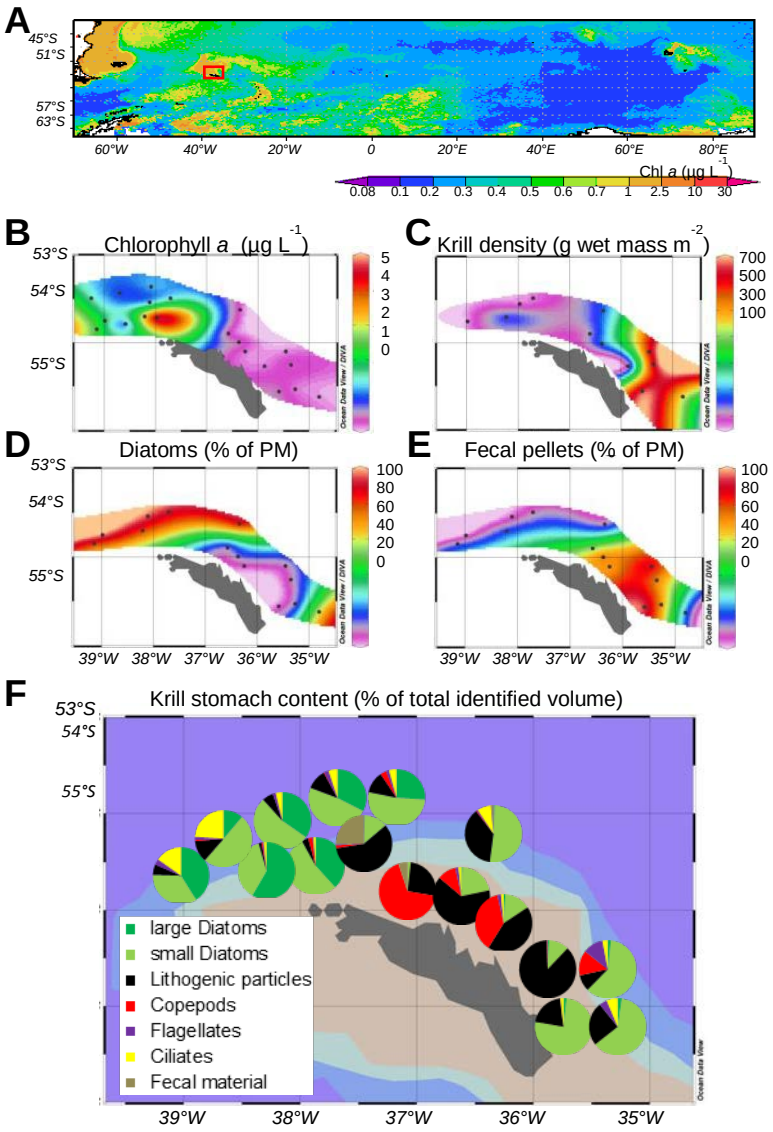

Figure 1 | Phytoplankton distribution and krill grazing at South Georgia (Southern Ocean). A, The Southern Ocean with the study area at South Georgia (red box) - overlaying a chlorophyll *a* (chl *a*) climatology derived from MODIS-Aqua (Jul 2002 - Feb 2015). **B-F,** Results from our study period: 25th Dec 2010 - 19th Jan 2011. **B,** Distribution of chl *a* (µg L^{-1}). **C,** Distribution of krill density (g wet mass m^{-2}). **D,** Proportion of diatoms in the suspended particulate matter (PM) at 20 m water depth. E, Proportion of fecal pellets in the suspended particulate matter at 20 m water depth. **F,** Stomach content of freshly-caught krill. (See also Fig. S1)

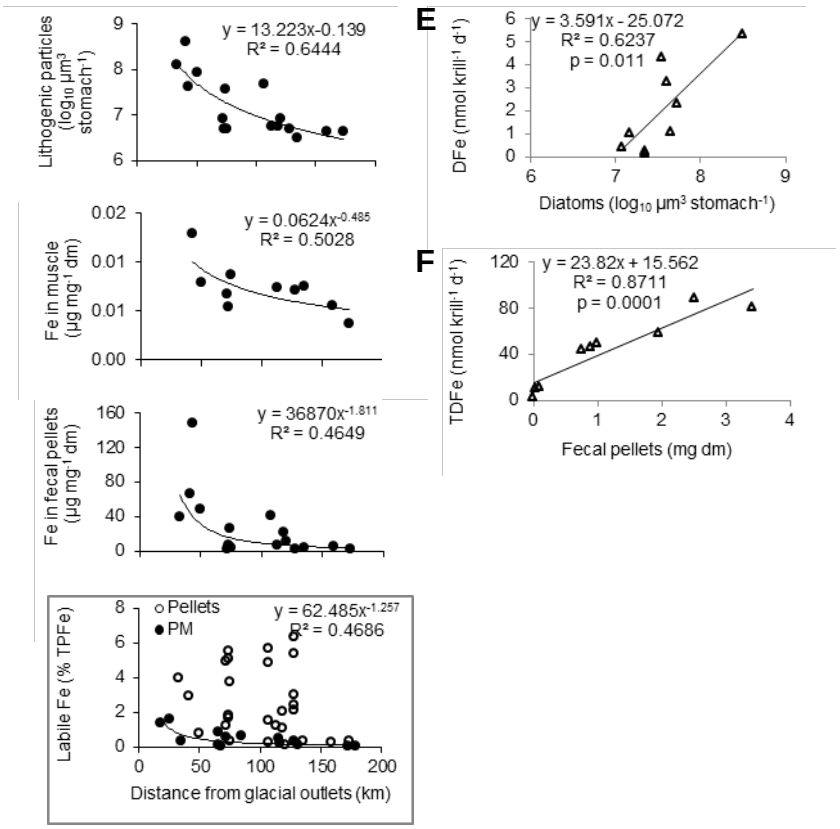

Figure 2 | Krill iron cycling.

A-D, Characteristics of freshly-caught krill in relation to the distance from major glacial outlets (Cumberland Bay). **A,** Volume of lithogenic particles in krill stomachs. **B,** Total particulate iron content in krill muscle tissue. **C,** Total particulate iron content in krill fecal pellets. **D,** Labile iron content in suspended particulate matter (PM) at 20 m water depth and in krill fecal pellets. dm - dry mass. TPFe – total particulate iron. **E-F,** Results from short-term shipboard incubations of freshly caught krill. **E,** DFe excretion rates in relation to the volume of diatoms in krill stomachs. **F,** TDFe release rates in relation to the dry mass of fecal pellets produced during 3h-incubations. (See also Table S2)

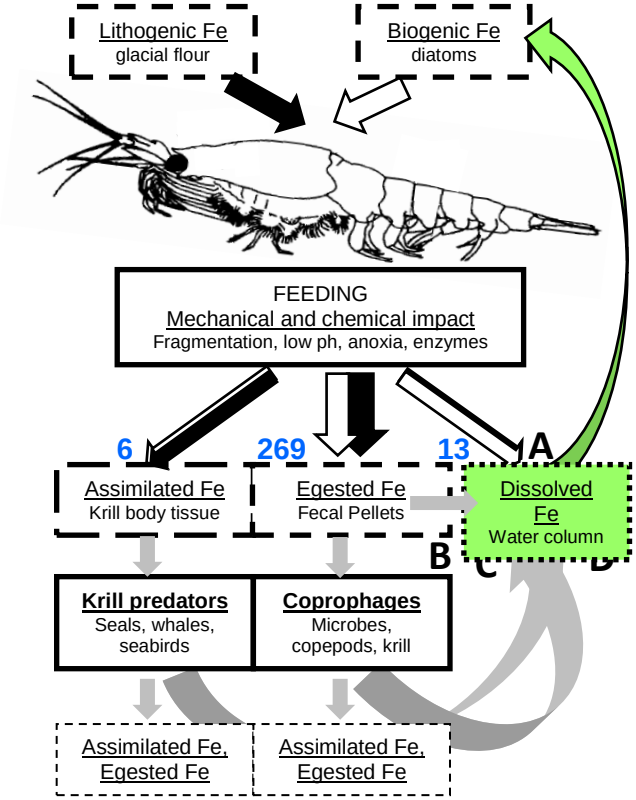

Figure 3 | Schema of iron flux through krill and pathways of DFe supply. Blue numbers indicate the partitioning of ingested iron between body tissue, fecal pellets and ambient water (nmol Fe g^{-1} dm d^{-1}). Black and open arrows schematically represent the relative fractions sourced from lithogenic- and biogenic iron respectively. Grey arrows indicate processes that remain to be quantified. In the upper mixed layer, iron ingested and mobilised by krill can lead to DFe supply via several pathways: A) Fragmentation and digestion of food by krill, B) Dissolution of particulate iron in fecal pellets due to photochemical reactions and complexation with ligands. C) Dissolution of particulate iron in fecal pellets due to microbial degradation and zooplankton coprophagy. D) Digestion of krill tissue by predators. (See also Table S3)

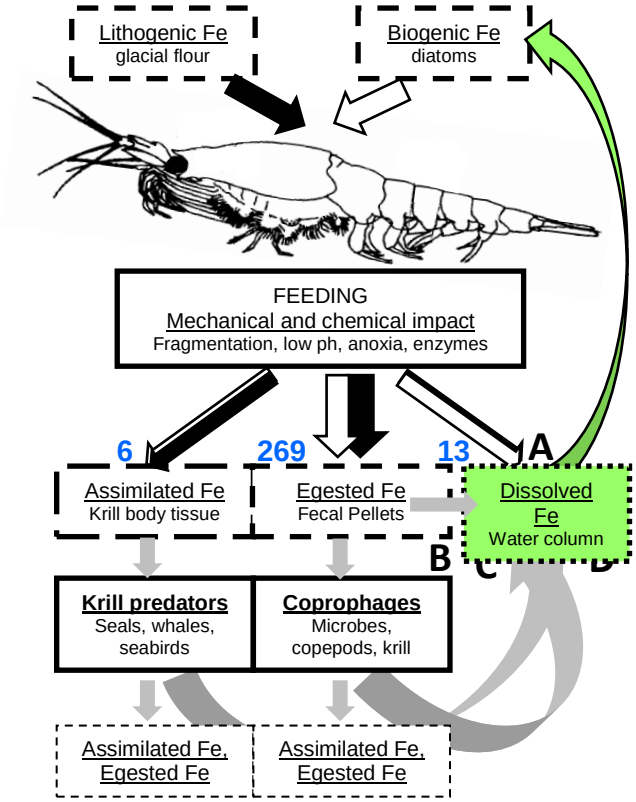

Figure 4 | Interannual differences in krill abundance as a predictor for chl *a* concentrations at South Georgia. A, Average chl *a* concentrations in years with low (left) and high (right) krill abundances on the South Georgia shelf. Years with low krill abundances: 2002/3, 2003/4, 2004/5, 2008/9, 2010/2011, 2012/2013. Years with high krill abundances: 2005/6, 2007/8, 2009/10, 2011/2012. **B**, Spatial distribution of negative (blue-purple) and positive (yellow-red) slope values for the regression between median chl *a* concentration and summer krill abundance at South Georgia for the years 2002-2013. Chl *a* concentrations were derived from ocean colour radiometry (MODIS 2002-2013, mid August-mid April, 8-day composites)**.** The black lines are drifter trajectories, which indicate that the surface current flow links the northern shelf of South Georgia to the main phytoplankton bloom area downstream with a transit time of 20-50 days [44]. (See also Fig. S2)

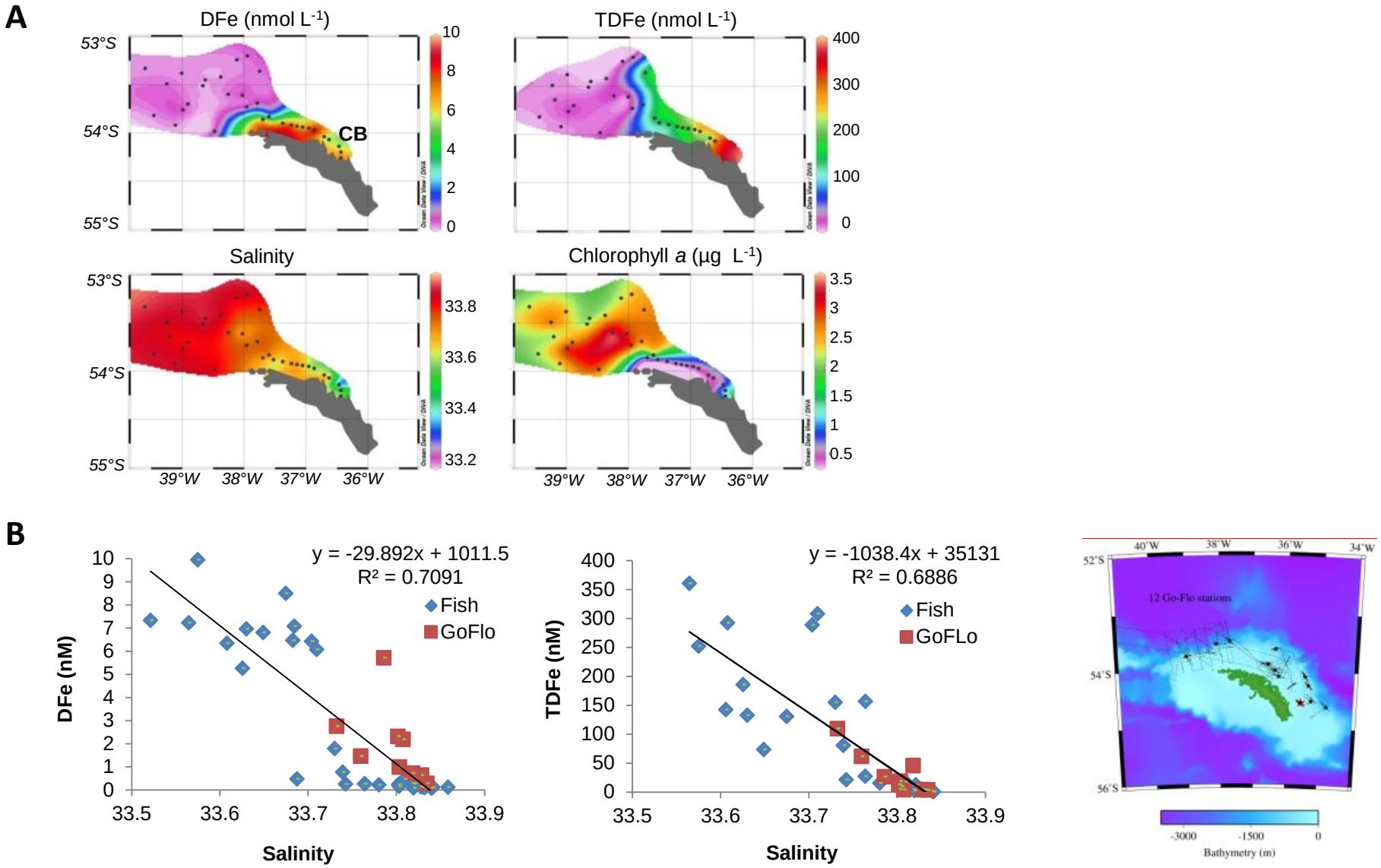

Fig. S1, Related to Fig. 1. Dissolved and total dissolvable iron concentrations north of South Georgia (study period: 25th Dec 2010 – 19th Jan 2011).
A, Concentrations of dissolved iron (< 0.2 µm, DFe) and total dissolvable iron (unfiltered, TDFe), salinity and chlorophyll *a* in surface waters from major glacial outlets at Cumberland Bay (CB) across the northern shelf and downstream of the island.. **B**, Relationship between DFe- and TDFe concentration and salinity in surface waters ('Fish', station locations in Fig. S1A) or at 20 m water depth ('GoFlo', station locations to the right).

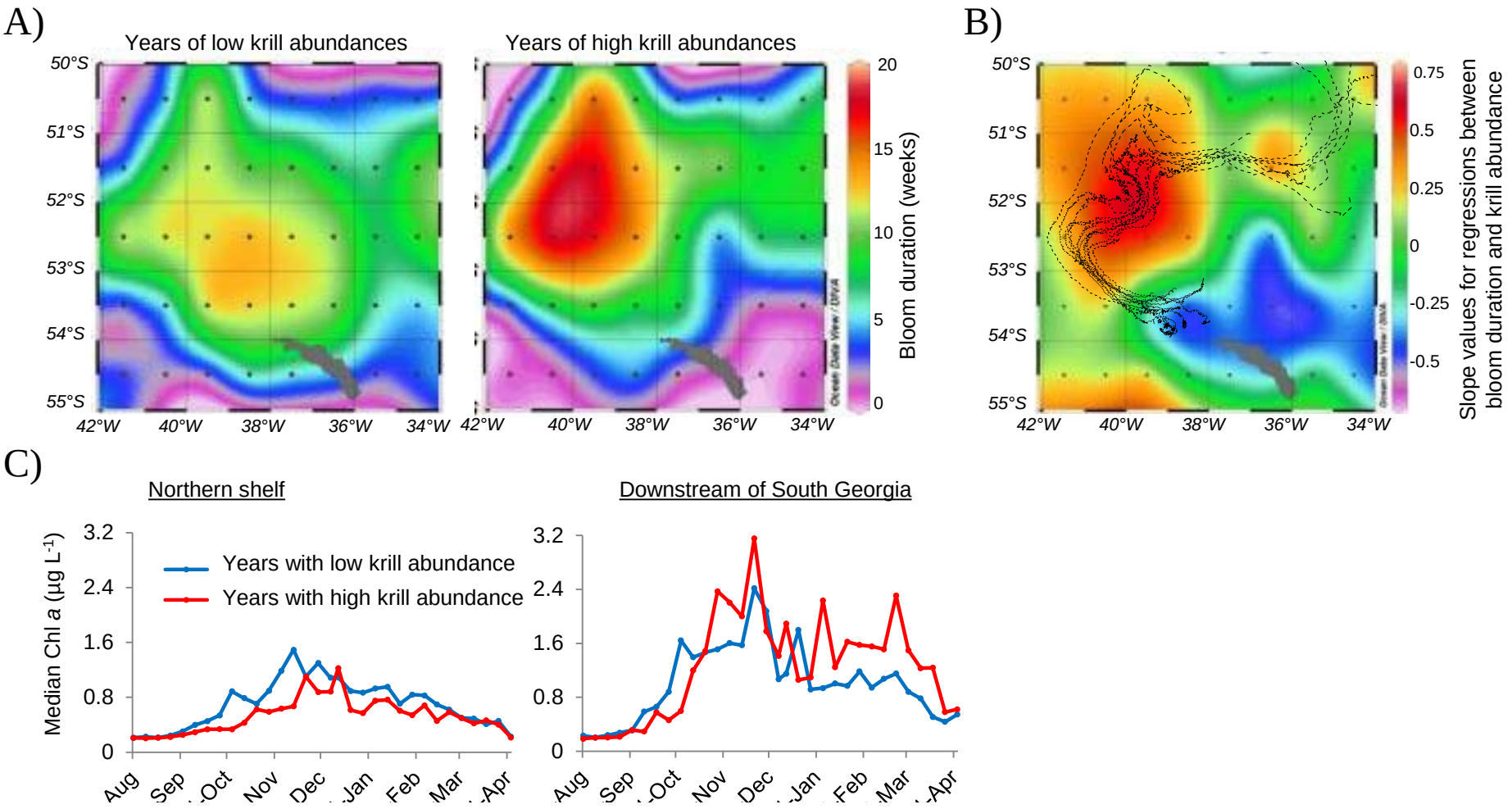

Fig. S2, Related to Fig. 4. Interannual differences in krill abundance as a predictor for the length of the phytoplankton bloom at South Georgia.
A) Average bloom length in years with low (left) and high (right) krill abundances at the South Georgia shelf. Years with low krill abundances: 2002/3, 2003/4, 2004/5, 2008/9, 2010/2011, 2012/2013. Years with high krill abundances: 2005/6, 2007/8, 2009/10, 2011/2012.
B) Spatial distribution of negative (blue-purple) and positive (yellow-red) slope values for the regression between median bloom length and summer krill abundance at South Georgia for the years 2002-2013. Chl *a* concentrations were derived from ocean colour radiometry (MODIS 2002-2013, mid August-mid April, 8-day composites)**.** A bloom was defined as ≥1 µg Chl *a* L^{-1}. The black lines are drifter trajectories, which indicate that the surface water current flow links the northern shelf of South Georgia to the main phytoplankton bloom area downstream with a transit time of 20-50 days [S1].
C) Time course of average annual chl *a* development on the shelf (left) and downstream of South Georgia (right) during years with low and high krill abundance . The right plot indicates that phytoplankton blooms downstream of South Georgia can extend into autumn in years with high krill abundance, but are restricted to spring and summer when the krill abundance is low.

Table S1, Related to Figure 2. Comparison between phytoplankton DFe demand and krill DFe supply for stations where the release of DFe by krill had been measured in ship-board incubations. blue – rates are expressed as per m^{-2} for the total upper ~300 m water column, red – rates are expressed as per m^{-3} for the upper mixed layer (45-70 m), green – results from ship-board incubations of krill.

	DFe-demand by phytoplankton					DFe-supply by krill					Percentage	
Event	Chl *a*	PP	DFe-demand-A	MLD	DFe-demand-B	DFe excretion	No krill-A	DFe supply-A	No krill-B	DFe supply-B	%	%
	(mg m^{-3})	(g C m^{-2} d^{-1})	(µmol Fe m^{-2} d^{-1})	(m)	(nmol Fe m^{-3} d^{-1})	(nmol Fe ind^{-1} d^{-1})	(ind m^{-2})	(µmol Fe m^{-2} d^{-1})	(ind m^{-3})	(nmol Fe m^{-3} d^{-1})		
17	2	0.46	1.43	60	23.8	5.3	185	0.98	1.4	7.4	69	31
44	1.3	0.36	1.12	60	18.6	1.1	185	0.2	1.4	1.5	18	8
67	1.5	0.39	1.21	60	20.1	3.3	130	0.43	0.9	3.0	35	15
92	0.26	0.21	0.65	70	9.4	4.3	1582	6.88	7.1	31	1050*	331*
107	0.26	0.21	0.65	70	9.4	0.1	1408	0.21	6.3	0.9	32	10
116	0.35	0.23	0.69	45	15.4	2.3	264	0.61	1.4	3.2	87	21
128	0.35	0.23	0.69	45	15.4	1.1	194	0.2	1.0	1.1	29	7
145	0.7	0.28	0.85	60	14.2	0.4	172	0.08	1.0	0.5	9	3
154	1	0.32	0.98	60	16.4	0.2	61	0.02	0.5	0.1	2	1
Mean	**0.9**	**0.3**	**0.9**	**59**	**15.9**	**2.0**	**464**	**1.1**	**2.3**	**5.4**	**35**	**12**

Calculations:
DFe-demand-A (µmol Fe m^{-2} d^{-1}) = Primary production (PP, g C m^{-2} d^{-1}) × Fe:C ratio (µmol mol^{-1})
DFe-demand-B (nmol Fe m^{-3} d^{-1}) = DFe-demand-A (µmol Fe m^{-2} d^{-1}) × 1000/ mixed layer depth (MLD, m)
DFe-supply-A (µmol Fe m^{-2} d^{-1}) = DFe-excretion rate (nmol Fe ind^{-1} d^{-1}) × No of krill-A (ind m^{-2})
DFe-supply-B (nmol Fe m^{-3} d^{-1}) = DFe-excretion rate (nmol Fe ind^{-1} d^{-1}) × No of krill-B (ind m^{-3})
No of krill-A (ind m^{-2}) = krill density (g m^{-2})/ krill dry mass (g ind^{-1})
No of krill-B (ind m^{-3}) = No of krill-A (ind m^{-2}) * percentage of krill in upper mixed layer (UML)]/ MLD (m)
/ - these values were exclude for the calculation of the mean value as they are exceptionally high

Assumptions: (1) PP at South Georgia can be calculated from Chl *a* values using the equation y = 144.59 x + 174.77, R^2 = 0.8322 (original data in [S2]).
(2) A Fe:C ratio of 37 µmol mol^{-1} is representative for natural phytoplankton populations under Fe-replete conditions [S3].

Krill density (g m^{-2}) and their vertical distribution across day- and night-time were estimated from acoustic backscattering. Average krill dry mass varied from 0.1 to 0.22 g ind^{-1} between stations.

Table S2, **Related to Figure 3.** Overview of iron measurements in krill tissue, fecal pellets and incubation water, and DFe supply from zooplankton feeding

Iron cycling through krill			**DFe supply from zooplankton feeding**
Particulate Fe (PFe)		**Dissolved Fe (DFe)**	(DFe release rate × biomass)
• PFe in tissue	➡	• DFe release from tissue	0.6-2.8 pM d^{-1} (copepods, [S8])
Muscle: 4-13 µg Fe g^{-1} dm [this study], [S4]		unknown	0.7-5.8 pM d^{-1} (mixed mesozooplankton, [S9])
Stomach: 0.03- 6 mg Fe g^{-1} dm [S4]			0.8-8 pM d^{-1} (micro- and mesozooplankton, [S10])
Whole krill: 4-174 µg Fe g^{-1} dm [S5], [S6]			0.1 – 31 pM d^{-1} (krill, [this study])
• PFe in fecal pellets	➡	• DFe release from pellets	31 pM d^{-1} (microzooplankton, [S11])
2-149 mg Fe g^{-1} dm [this study]		unknown	17-115 pM d^{-1} (microzooplankton, [S12])
• TDFe release when feeding	➡	• DFe release when feeding	
0.02-0.6 µmol TDFe g^{-1} dm d^{-1} [this study]		0.9-34 nmol DFe g^{-1} dm d^{-1} (this study)	**DFe supply from fecal pellets**
0.5-16.5 µmol TDFe g^{-1} dm d^{-1} [S7]			6-96 pM d^{-1} (copepods, [S12])

Calculation of TDFe- and DFe release rates were based on a krill dry mass (dm) of 0.156 g ind^{-1}, which represents an average value for the sampling stations of this study.

Supplemental Experimental Procedures (I)

Cruise details. This study was part of a research expedition to the northern shelf of South Georgia from 25th December 2010 to 19th January 2011 onboard RRS *James Clark Ross*.

Temperature, salinity and fluorescence. Vertical profiles of conductivity-temperature-depth (CTD) and fluorescence were collected with a SeaBird Electronics 9 Plus (SBE 9Plus) CTD and attached Aqua Tracka fluorometer (Chelsea Instruments). Underway surface salinity and fluorescence were obtained from the Oceanlogger SBE45 CTD using the ship's seawater supply. Non-calibrated fluorescence data are given in 'relative units'.

Abundance of diatom, flagellates, ciliates and bacteria . At each station, discrete water samples for taxonomic analysis of the plankton community were taken from 20m depth with a 10L Niskin bottle on a standard stainless steel CTD rosette. Samples were preserved with 2% acidic Lugol's solution and stored in 250 ml amber glass bottles. A 50 ml sub-sample was settled for 24h in an Utermöhl counting receptacle and examined with an inverted microscope (Zeiss, Axiovert 25). Rare items (i.e. large diatoms, thecate dinoflagellates and large ciliates) were counted by scanning the complete receptacle at × 200 magnification, while small common items were enumerated from two perpendicular transects across the whole diameter of the receptacle. The smallest items included in this study were approximately 5 µm. Autotrophic flagellates, small naked dinoflagellates and thecate dinoflagellates were grouped as 'flagellates'. The dimensions of the different taxa were measured and the volume calculated based on simple geometric shapes or combinations thereof [S13].

Composition of suspended particulate matter. Stand-Alone Pumping Systems (SAPS, Challenger Oceanic) were deployed to sample suspended particulate matter from 20m, 50m and 150m water depth. Material was pumped for 1-1.5 hours and filtered onto polycarbonate filters (293 mm diameter, 1 µm pore-size, Sterlitech, USA). From each filter a small piece (~5 cm^2) was cut out with a ceramic knife for subsequent microscopical examination. The remaining filter was stored at -20°C for trace metal analysis. The microscopical analysis was carried out in analogue to that of plankton samples obtained with the Niskin bottles. However, due to the larger volume (mean: 530±210 L) and greater water depth, SAPs samples contained additional items such as copepods, nauplii, pteropods, tintinnids, fecal pellets and lithogenic particles. All items were enumerated and their dimensions measured. The volume and carbon content of copepods was estimated from their prosome length, that of nauplii from the total length according to [S14]. The shape of other items was considered to be either spherical (pteropods, some fecal pellets), cylindrical (fecal pellets) or a truncated cone (tintinnids). Due to intermediate size or breakage, fecal material (≥ 25 µm diameter) was combined into one category regardless its origin from copepods, euphausiids or pteropods. Lithogenic particles were counted in 3 size fractions: 5-10 µm, 11-25 µm and 26-50 µm and the volume was considered to be equal to a half-sphere.

Krill acoustics. Krill density (g m^{-2}) and their vertical distribution were estimated from acoustic backscattering according to [S15]. The mean krill density per station was calculated from multiple 10-nm-transects across the area. Usually 5-7 transects were run to span a diel cycle. By pooling day-time *vs.* night-time transects, patterns in krill diurnal vertical migration were extracted. For the conversion of krill density (g m^{-2}) into carbon concentrations (mg C m^{-3}), first, the average wet mass of krill in the upper 50 m water column was calculated using day- and night-time vertical distribution profiles and, second, wet mass was transferred into carbon content applying a multiplication factor of 0.0993 [S16].

Live krill sampling was based on targets identified with the echosounder and carried out with purpose-built 1 m^2 square nets. To allow for short duration hauls, all but one of the targets were in the upper 50 m water column. Solid plastic cod ends minimised abrasion to the catch. Onboard, krill were immediately transferred into the cold room (2°C). A batch of ~50 krill was frozen at -80°C for diet analysis and trace metal analysis of muscle tissue.

Krill stomach content. To examine krill diet, the stomach was dissected from frozen krill and samples were analysed according to [S4],[S13].

Fecal pellet collection. About 150-200 healthy individuals were sequentially washed in a series of acid-cleaned buckets filled with 0.2 µm-filtered seawater obtained from trace metal clean towed fish and then left for defecation in a laminar flow cabinet in a temperature-controlled room (2°C). Fecal pellets were collected at 0.5-1 h intervals over a maximum of 3 hours using acid washed plastic pipettes. The pellets were purified, transferred to an acid washed plastic tube, rinsed twice with deionised water (Milli-Q, Millipore) and then frozen at -80°C for subsequent analysis of trace metals.

Supplemental Experimental Procedures (II)

Krill bottle incubations. To set up the experiments, water from towed (2-3 m depth) trace metal clean fish was passed through a 0.2 µm membrane filter in a class 100 laminar flow cabinet and filled sequentially into 4-5 acid-washed 9 L-polycarbonate (PC) carboys (Nalgene). The carboys were placed in a laminar flow cabinet in a temperature-controlled room (2°C). Krill were first sequentially washed in three 5 L acid cleaned plastic buckets containing 0.2 µm filtered seawater and then placed into 2-3 of the 9 L PC carboys (10-20 krill carboy^{-1} depending on their body size). The other 2 PC carboys served as controls. After initial mixing and adding krill, a subsample of 120 ml water was taken from each carboy tap and subsequently after 1 h and 3 h. The samples were transferred to a trace metal clean laboratory container for the analysis of DFe and TDFe. Following the termination of the experiments, the fecal pellets remaining at the bottom of the carboys were quantitatively collected into an acid washed plastic tube, twice rinsed with deionised water and then frozen at -80°C. The krill used in the experiments were also frozen at -80°C for subsequent enumeration and morphometric measurements.

Dissolved iron (DFe) and total dissolvable iron (TDFe) in water samples. Discrete water samples were collected from depths between 20-1000 m using six trace metal clean GO-FLO bottles (General Oceanics, Miami, USA) deployed on a Kevlar wire. In addition, surface water samples for DFe and TDFe were collected using the towed fish. The surface water was pumped from the towed fish to the trace metal clean laboratory container via an enclosed system, using Teflon tubing and suction provided by a peristaltic pump (Watson Marlow). Samples for DFe measurements were filtered through 0.2 µm cartridge filters (Sartobran P300, Sartorius) with gentle N_2 overpressure. The filtration was carried out in a class 100 laminar flow hood. Both DFe and TDFe samples were stored in 125 mL acid-washed low density polyethylene bottles (LDPE, Nalgene), acidified with ultra pure HNO_3 (Romil UpA) to pH 1.66 (22 mmol H^+L^{-1}), and shipped to the National Oceanography Centre Southampton (NOCS). For off-line preconcentration of DFe and TDFe an automated system (Preplab) with a WACO preconcentration/matrix removal resin [S17] was used. Concentrations of DFe and TDFe were determined by isotope dilution inductively coupled plasma – mass spectrometry (ID-ICP-MS, Element II XR ThermoFisher Scientific) according to the method described by [S18].

It should be noted that TDFe represents DFe plus the amount of Fe re-dissolved from particles following > 6 months sample storage after the addition of 22mmol H^+ L^{-1}. This implies that acid-inert minerals (e.g. zircon) and their associated trace metals likely did not contribute to the total dissolvable concentration. The analytical blank of the ICP-MS method was determined and showed that the acid blank (distilled HNO_3) was negligible, while the buffer blank (2M NH_4Ac pH8.9) did not exceed 0.06 nmol L^{-1}. The detection limit of this method was 0.03 nmol L^{-1} (defined as three times the standard deviation of the system blank, n = 3). The accuracy of the system was assessed by the determination of DFe in surface water (SAFe S) and deep water (SAFe D2), collected during the SAFe programme and in GEOTRACES surface (GS) and deep (GD) seawater reference materials. The concentration of DFe measured during this study was SAFe S = 0.087 ± 0.025 nmol L^{-1} (n = 25), SAFe D2 = 0.90 ± 0.10 nmol L^{-1} (n = 19), GEOTRACES GD = 1.28 ± 0.15 nmol L^{-1} (n = 3), and GS = 0.56 ± 0.05 nmol L^{-1} (n = 6). All standard seawater values were in good agreement with the census values (SAFe S = 0.093 nmol L^{-1}; SAFe D2 = 0.93 nmol L^{-1}, GS = 0.55 nmol L^{-1}; GD = 1.00 nmol L^{-1}).

Particulate iron in suspended material, krill fecal pellets and krill muscle tissue. Suspended particles were collected by the Stand-Alone Pumping Systems attached to a Kevlar wire and deployed for 1.-1.5 h at 20 m, 50m, and 150 m. Acid cleaned 1 µm polycarbonate filters (Sterlitech, 293 mm diameter) were mounted and demounted in the individual filter holders in a laminar flow hood. The PC filters were stored at -20°C and shipped frozen to the NOCS. Here, filters were thawed and particles were rinsed off using deionized water. Particles were collected on acid cleaned 47 mm PC filters (0.4µm poresize, Sterlitec) mounted in a polytetrafluoroethylene (PTFE, Nalgene) filter holder. Following filtration, the loaded filters were transferred into a 50 mL acid cleaned PTFE container. The labile particulate trace metal fraction was remobilized using a 25% acetic acid solution (SpA, Romil) over a period of three hours. Subsequently, the filters were transferred carefully into acid cleaned petri dishes (Fisher) and particles removed from the filters during the leaching process in the 50 ml PTEE containers were concentrated by centrifugation. The remaining 25% acetic acid solution was decanted into 25 mL acid cleaned PTFE containers.

Supplemental Experimental Procedures (III)

The acetic acid solution was evaporated to dryness on a heat plate set to 90°C. The remaining salts were re-dissolved by 1 mL of concentrated sub-boiled HNO_3 (PTFE still, Savilex). The solution was concentrated on the heat plate until a small drop of HNO_3 was left. This drop was diluted with 10 mL of 2% HNO_3 (sub-boiled) and transferred into 30 mL acid cleaned LDPE bottles and stored until analysis.

After decanting the 25% acetic acid solution, the wet 47 mm PC filters were transferred back into the 50 mL PTFE container and placed onto the PTFE container wall to minimize the filter blank. To digest the remaining particles, 2 mL of concentrated sub-boiled HNO_3 and HCl (PTEE still, Savilex) and 13 drops of concentrated hydrofluoric acid (HF, SpA, Romil) were added. The PTFE container was closed and placed on a heat plate at 140°C. After 4 hours the container was carefully opened and the HNO_3/HCl/HF solution was evaporated to dryness. The undigested filters were removed and the remaining salts were re-dissolved with 2 mL concentrated sub-boiled HNO_3 and evaporated on the heat plate until a small drop of HNO_3 was left. This drop was diluted with 15 mL of 2% HNO_3 (sub-boiled) and transferred into 30 mL acid cleaned LDPE bottle until analysis. All samples were analyzed by ICP-MS (Thermo Fisher Scientific, X-Series) using calibrations by standard additions and In/Re for drift control. Particulate iron concentrations (PFe) in the water column were determined by applying the water volume recorded by the flowmeter on the SAPs and hence had passed the SAPs PC filter. The leaching and digestion of krill fecal pellets and krill muscle tissue were performed in a similar manner as described for the SAPS particles.

To validate the determined trace metal concentrations, certified reference materials (HISS-1, NIST 1573a, NIST 1648a, TORT-2) were analysed with each batch of samples. Results were in good agreement with certified values (HISS-1: 2.54±0.50 g kg^{-1} (2.50 g kg^{-1}); NIST 1573a: 0.38±0.01 g kg^{-1} (0.37 g kg^{-1}); NIST 1648a: 37.5±4.4 g kg^{-1} (39.2 g kg^{-1}); TORT-2: 0.12±0.00 g kg^{-1} (0.11 g kg^{-1})). The limit of detection (defined as three times the standard deviation of the system blank n = 3) did not exceed 0.2 µg kg^{-1}, and the blank of the method was below the limit of detection (LOD).

Phytoplankton bloom characteristics. Chlorophyll *a* (chl *a*) concentrations were obtained from ocean colour radiometry (MODIS, 2002-2014, 9 km standard product, 8-day composites, 20th of August – 20th of April). Therefore the area of the South Georgia bloom (50°S-55°S, 34°W-42°W) was divided into 40 subareas of 1°Lat x 1°Lon. For each of these subareas the annual median chl *a* concentration and bloom duration (chl *a* ≥1µg L^{-1}) were determined. During the years 2006/7 and 2013/14 no proper phytoplankton bloom developed at South Georgia, and therefore these years were excluded from further analysis.

Annual krill abundance at South Georgia. As an index of the annual krill abundance at SG we used the inverted anomaly of the median krill body length for the years 2002/3, 2003/4, 2004/5, 2005/6, 2007/8, 2008/9, 2009/10, 2010/11, 2011/12, 2012/13. The krill body length data derived from a long-term dietary analysis of Antarctic fur seals based on weekly collected scat samples [S19]; the raw data are available on request from the British Antarctic Survey. Here we calculated the annual median krill body length from scat samples collected during austral summer (beginning of December to end of February). About 1000 krill were measured for each of the years. The occurrence of small krill at South Georgia (median length <50 mm in predator diet) is associated with successful krill recruitment and transfer from nursery areas further south [S20]. Moreover, the dominance of smaller krill also indicates high mass-specific feeding rates [S21], which further enhances the effect of a large population on the food environment. In contrast, the dominance of large krill (>50mm) indicates an aging population with low influx of younger krill [S20] and low mass-specific feeding rates [S21], and therefore less impact on the food environment.

Supplemental References

S1 Meredith, M.P., Watkins, J.L., Murphy, E.J., Cunningham, N.J., Wood, A.G., Korb, R., Whitehouse, M.J., and Thorpe, S.E. (2003). An anticyclonic circulation above the Northwest Georgia Rise, Southern Ocean. Geophys. Res. Lett. *30(20)*, 2061. doi: 10.1029/2003GL018039.

S2 Korb, R.E., and Whitehouse, M.J. (2004) Contrasting primary production regimes around South Georgia, Southern Ocean: large blooms versus high nutrient, low chlorophyll waters. Deep-Sea Res. I *51*, 721-738 (2004).

S3 Twining, B.S., Baines, S.B., Fisher, N.S., and Landry, M.R. (2004) Cellular iron contents of plankton during the Southern Ocean Iron Experiment (SOFeX). Deep Sea Res. I *51*, 1827-1850.

S4 Schmidt, K., Atkinson, A., Steigenberger, S., Fielding, S., Lindsay, M.C.M., Pond, D.W., Tarling, G., Klevjer, T.A., Allen, C.S., Nicol, S., and Achterberg, E.P. (2011). Seabed foraging by Antarctic krill: implications for stock assessment, bentho-pelagic coupling and the vertical transfer of iron. Limnol. Oceanogr. *56*, 1411-1428.

S5 Palmer Locarnini, S.J..P, and Presley, B.J. (1995) Trace element concentrations in Antarctic krill, *Euphausia superba*. Polar Biol. *15*, 283-288.

S6 Nicol, S., Bowie, A., Jarman, S., Lannuzel, D., Meiners, K.M., and van der Merwe, P. (2010). Southern Ocean iron fertilization by baleen whales and Antarctic krill. Fish and Fisheries *11*, 203-209.

S7 Tovar-Sánchez, A., Duarte, C.M., Hernández-León, S., and Sañudo-Wilhelmy, S.A. (2007). Krill as a central node for iron cycling in the Southern Ocean. Geophys. Res. Lett. *34*, L11601, doi:10.1029/2006GL029096.

S8 Sarthou, G., *et al.* (2008) The fate of biogenic iron during a phytoplankton bloom induced by natural fertilisation: Impact of copepod grazing. Deep-Sea Res. II *55*, 734-751.

S9 Giering, S.L.C., Steigenberger, S., Achterberg, E.P., Sanders, R., and Mayor, D.J. (2012) Elevated iron to nitrogen recycling by mesozooplankton in the Northeast Atlantic Ocean. Geophys. Res. Lett. *39*, L12608.

S10 Bowie, A.R., et al. (2001) The fate of added iron during a mesoscale fertilisation experiment it the Southern Ocean. Deep-Sea Res. II *48*, 2703-2743.

S11 Strzepek, RF., *et al*. (2005) Spinning the 'Ferrous Wheel': The importance of the microbial community in an iron budget during the FeCycle experiment. Glob. Biogeochem. Cyles *19*, GB4S26.

S12 Boyd, P.W., Strzepek, R., Chiswell, S., Chang, H., DeBruyn, J.M., Ellwood, M, Keennan, S., King, A.L., Maas, E.W., Nodder, S., et al. (2012). Microbial control of diatom bloom dynamics in the open ocean. Geophys. Res. Lett. *39*, L18601.

S13 Schmidt, K., Atkinson, A., Petzke, K.-J., Voss, M., and Pond, D. W. (2006) Protozoans as a food source for Antarctic krill: complementary insights from stomach content, fatty acids, and stable isotopes. Limnol. Oceanogr. *51*, 2409-2427.

S14 Mauchline , J. (1998). The biology of calanoid copepods. Adv. Mar. Biol. 33, 1-710.

S15 Fielding, S. *et al.* (2014) Interannual variability in Antarctic krill (*Euphausia superba*) density at South Georgia, Southern Ocean: 1997-2013. ICES J Mar Sci. doi:10.1093/icesjms/fsu104.

S16 Atkinson, A., Ward, P., Hunt, B.P.V., Pakhomov, E.A. , and Hosie, G.W. (2012) An overview of Southern Ocean zooplankton data: Abundance, biomass, feeding and functional relationships. CCAMLR Science *19*, 171-218.

S17 Kagaya, S. *et al.* (2009) A solid phase extraction using a chelate resin immobilizing carboxymethylated pentaethylenehexamine for separation and preconcentration of trace elements in water samples. Talanta *79*, 146-152.

S18 Milne, A., Landing, W., Bizimis, M., and Morton, P. (2010) Determination of Mn, Fe, Co, Ni, Cu, Zn, Cd and Pb in seawater using high resolution magnetic sector inductively coupled mass spectrometry (HR-ICP-MS). Anal. Chimi. Acta *665*(2), 200-207.

S19 Reid, K. (1995) The diet of Antarctic fur seals (*Arctocephalus gazelle* Peters 1875) during winter at South Georgia. Ant. Sci. *7*, 241-249.

S20 Forcada, J., and Hoffman, J. I. (2014) Climate change selects for heterozygosity in a declining fur seal population. Nature *511*, 462-465.

S21 Schmidt, K., and Atkinson, A (2016) Feeding and food processing in Antarctic krill (*Euphausia superba* Dana), In V. Siegel (ed.) 'Biology and Ecology of Antarctic Krill'. Advances in Polar Ecology. Springer, Dortrecht. DOI 10.1007/978-3-319-29279-3_5